Structure and energetics of the vacancy in graphite

A. A. El-Barbary,[1,*] R. H. Telling,[1] C. P. Ewels,[1,2] M. I. Heggie,[1] and P. R. Briddon[3]
[1]*CPES, University of Sussex, Falmer, Brighton, BN1 9QJ, United Kingdom*
[2]*Laboratoire de Physique des Solides (UMR CNRS 8502), Building 510, Paris Sud, Université 91405 Orsay, France*
[3]*Physics Centre, School of Natural Science, Newcastle upon Tyne, NE1 7RU, United Kingdom*
(Received 21 February 2003; revised manuscript received 22 May 2003; published 15 October 2003)

We determine properties of the vacancy in graphite from first principles calculations. The ground-state structure is associated with a formation energy of 7.4 eV and arises through a combination of symmetric relaxation and symmetry-breaking Jahn-Teller distortion to one of three degenerate, symmetry-related structures. The distortion results in a weak reconstructed bond and small out-of-plane atomic displacements. Dynamic switching between degenerate structures is activated by a barrier of 0.1 eV and we interpret scanning tunneling microscopy observations on the basis of thermal averaging between structures. The calculated migration energy of 1.7 eV is lower than that widely accepted from experiment, and we propose that the discrepancy is explained by a revised picture of trapping during vacancy transport, dependent on concentration. We discuss the significance of these findings in understanding defect behavior in irradiated graphite and related graphitic materials, in particular single-walled nanotubes.

DOI: 10.1103/PhysRevB.68.144107 PACS number(s): 61.72.Ji, 61.80.Az, 81.05.Uw, 28.41.Pa

I. INTRODUCTION

The interest in point defects in graphite originates in a number of research fronts. Apart from purely academic investigation, defect studies in graphite and graphitic materials were first motivated by the desire to understand aspects of radiation damage occurring in graphite-moderated nuclear reactors.[1] Characterization of atomic-scale surface structure is also an important research drive, since graphite is a common substrate for use in various microscopy techniques.[2] Furthermore, the emerging field of carbon nanoscience[3] draws much useful information from the basic graphite system and for the large part shares behavior in common including defect structure and energetics (notwithstanding small effects due to curvature). Vacancy defects arise in graphite at low concentrations[4] during defective growth or as part of the thermal equilibrium concentration. They are much more prevalent in irradiated materials and are believed to be the predominant defects on irradiated graphite surfaces[5] and in nanotubes. Theoretical studies of the vacancy in graphite are an important and fundamental contribution to understanding the basic and complex defect processes in these materials. The work here aims to develop a more detailed understanding of vacancy structure and energetics.

Previous studies on the vacancy in graphitic systems have included both theoretical and experimental work. Experimental investigations include scanning tunneling microscope (STM), positron annihilation spectroscopy, and transmission electron microscope (TEM) studies.[4,6–8] STM measurements have provided most information on the monovacancy, although a straightforward interpretation of these results is hampered by probe-tip interactions[6] and scan rate, which we discuss in more detail later. Theoretical treatments have previously been given at various levels: simple bond-energy calculations of the formation energy,[9,10] a more advanced two-dimensional defect-molecule approach[11–13] incorporating Hückel theory to obtain the loss in energy due to interruption of the π-electron system, a charge self-consistent extended modified Hückel theory with semi-empirical configuration interactions,[14] embedded cluster with complete neglect of differential overlap (CNDO)-theory level,[15] extended Hückel theory using a semiempirical valence-effective Hamiltonian,[16] a tight-binding interatomic potential model,[17] and first principles theory using local density functional theory.[18] Using tight binding molecular dynamics simulations in 2000 Krasheninnikov *et al.*[19] reported the formation of asymmetric vacancies, a 5-1db defect (pentagon-one dangling bond) on walls of carbon nanotubes. This 5-1db defect has a lower energy than the other defects considered symmetric vacancy defect and 5–6 defect (four-fold coordinated atoms in the center of two pentagons and two hexagons). They suggested that such defects may survive at low temperature for times which may be long enough for experimental detection. Despite the attention paid to this single defect, constraints in calculational flexibility and accuracy have limited the knowledge gained thus far and, as we shall see, some important subtleties in behavior have been missed.

II. METHODOLOGY

The defect system we model consists of a central vacant atomic site within a region of lattice sufficiently extended to minimize boundary effects on the energies of interest. Graphite is highly anisotropic in structure and properties, meaning that for many purposes we can separate out in-layer and cross-layer interactions. It is also computationally efficient to model the vacancy in a noninteracting graphene sheet rather than graphite itself. An atomic cluster description of the defect system is used, based on hydrogen-terminated graphene sheets (polycyclic aromatic hydrocarbons, PAH), $C_{111}H_{26}$ with C_{2v} symmetry and $C_{120}H_{27}$ and $C_{190}H_{37}$ with D_{3h} symmetry, all having a central vacant site. We found that these are of a sufficient size that the formation energies are converged to within 0.01 eV. We adopt a first principles approach with AIMPRO code[20] where the total energy solutions to the many-particle Schrödinger equation for these systems are found within the density functional formalism[21,22] in a

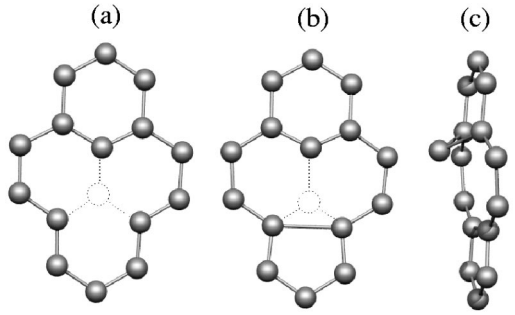

FIG. 1. (a) The fully optimized structure of locality of the symmetric D_{3h} vacancy, $C_{120}H_{27}$. (b) and (c) are the top and side views of the fully optimized structures of the distorted vacancy, $C_{120}H_{27}$, respectively.

Gaussian basis. Exchange and correlation are treated in the local density approximation. Norm-conserving pseudopotentials are used for the electron-ion interaction,[23] and minima in the total energy are obtained using a conjugate gradient algorithm. A basis set of Gaussians with four exponents is used to represent the *s*- and *p*-like atomic orbitals. The charge density is fitted to four *s* Gaussians for C and three for H. The systems were assumed to be electrically neutral. Charge density oscillations in part-filled degenerate orbitals during the self-consistency cycle were damped using a Fermi occupation function with $k_BT=0.02$ eV. Here we report spin averaged, cluster calculations. In this work, we have chosen to locate saddle points by symmetry where possible or otherwise by constructing the vector difference between the relaxed initial and final states, and stepping along this vector while optimizing all atomic movement orthogonal to it. In our simulation of the STM, charge density is calculated in such a way that the distance between the surface and the tip is kept constant, at 1 Å (constant height mode). Experimentally, to obtain a two-dimensional STM image, the current between the surface and the tip is normally kept constant during the scan of the surface (constant current mode). Once the equilibrium structures are obtained, we obtain the wave functions for the desired energy levels, close to the Fermi level, and the charge densities are calculated.[24] The images are generated for an applied voltage V such that all wave functions with energy levels within the energy range $E_f \rightarrow E_f+V$ are taken, squared and summed, to give a partial charge density. It is a slice through this charge that we take to generate our STM images.

III. RESULTS AND DISCUSSION

A. Vacancy structures

Following earlier work on the vacancy,[11,13] it was anticipated that the ideal, D_{3h} neutral vacancy with doubly degenerate $2E'$ σ states, undergoes a Jahn-Teller distortion, splitting this state in order to lower the total energy. We found that this distortion gives an energy lowering of around 0.2 eV, partitioned into terms due to the in-plane reconstruction (0.09 eV) and the out-of-plane displacement (0.10 eV). These geometries are given in Fig. 1. In the symmetric vacancy [Fig. 1(a)], the bond length between the first nearest-neighbor to the vacancy and the next-nearest neighbors is shortened to 1.37 Å where the nearest-neighbor bond length in perfect graphite is ~1.41 Å. This symmetry preserving distortion lowers the energy by 0.07 eV. Other bond lengths are slightly altered. For the distorted ground state, note the formation of a closed five-fold ring on reconstruction [Fig. 1(b)] as a result of the reconstructed bond of length 2.1 $\pm$0.1 Å (the range arises from a small dependence on cluster size). We would thus characterize this bond as weak and the reconstruction as a whole relatively minor in energetic terms (0.2 eV; see above). However, although the net reconstruction energy of the total system is small, an indication of the local bond strength and large motivation for reconstruction is that it has distorted a significant portion of the surrounding lattice at a cost in strain energy. This strain defeats a fuller reconstruction in the case of an infinite graphene sheet. The charge density at the midpoint between the atoms (previously second-nearest neighbor) is around one electron per $Å^3$ as compared with effectively 0 before reconstruction and just over two electrons per $Å^3$ between nearest-neighbor atoms. A qualitative understanding of the out-of-plane displacement is that the paired electrons in the new bond repel the electron on the atom opposite; the easiest direction for movement is an out-of-plane displacement. In addition, there is an elastic effect mediated by the lattice: the contraction caused by reconstructions is transmitted to the neighbors of the dangling bond atom, forcing them together. The dangling bond atom, in order to preserve its bond lengths moves out of the plane [by $\Delta z \sim 0.47$ Å bringing its two neighbors with it by $\Delta z \sim 0.24$ Å; see Fig. 1(c)].

Substantially the same ground-state structure was also obtained when using a local-spin-density functional on the cluster system and further, when adopting a supercell representation with periodic boundary conditions ($4\times4\times1$ unit cells plus vacancy=63 atoms). Supercell functionality was available in the AIMPRO code, again using a Gaussian basis and the structure was separately verified with the CASTEP code,[25] which employs a plane-wave basis (310-eV cutoff used). Spin-polarized calculations, for the odd-alternant, $C_{120}H_{27}$ ($s=1/2$), and even alternant systems, $C_{111}H_{26}$ ($s=0$) systems, and for the supercell system ($s=1$) show that the spin-polarized state is higher in energy by approximately 0.5 eV and we therefore conclude that the ground-state vacancy in graphite is spin free.

To see how curvature could affect the behavior of the vacancy defect in a nanotube, we took the graphene sheet $C_{120}H_{27}$ having a central vacant site and curved it slightly (radius of 15 Å) before relaxing it. The reconstruction bond (~1.8 Å) and the displacement of the remaining dangling carbon atom out of the graphene sheet occurred spontaneously. Therefore, when the atomic layer is strongly curved such as in a nanotube or fullerene, the reconstructed bond is expected to be much shorter since the second-nearest-neighbor distance is slightly shorter, the π bonding is weakened due to the lessened overlap of the p_z orbitals and the curvature will give the partially bound atom a natural bias out of plane to start with.

B. Wave functions and energy levels

1. A simple model: Hückel theory

Hückel theory is a good starting point for discussing the molecular orbitals (MOs) of the polycyclic aromatic hydrocarbons (PAHs) that we use to model graphene. We preserve the symmetry of the ideal vacancy using a D_{3h} cluster $C_{121}H_{27}$ in the *xy* plane. Being an odd alternant system, this is a π radical whose nonbonding orbital (of energy α) resides on every other carbon atom-choosing the set of carbon atoms with the greatest number of under-coordinated p_z orbitals. One way of interpreting this orbital is that it belongs to the two fold degenerate state at *K* in the graphene Brillouin zone—the first of these states resides on every other atom, and the second on the remaining atoms. Treating the ''empty'' atom sites surrounding the cluster as sites of repulsive potential, (i.e., zero rather than α, where α is a negative quantity), the state which remains is that which resides on most atoms. Interesting features of this cluster are the two large accidental degeneracies (fivefold) at $E=\alpha\pm\beta$, where β is the bonding parameter (''resonance integral'') in Hückel theory. This appears to derive from the van Hove singularities apparent in the graphene density of states from the two bands, $E=\alpha\pm\beta$ at *M*. Indeed these states at *M* comprise zig-zag chains, which are common to MOs in our clusters at $E=\alpha\pm\beta$. Furthermore, the hydrogenated zig-zag edges of our cluster also give rise to high density states near the Fermi level, as they do in ribbons.[26]

In Hückel theory, introduction of the vacancy to this cluster eliminates the π radical, introduces a highest occupied—lowest unoccupied molecular orbital (HOMO-LUMO) gap of -0.256β and reduces the resonance energy by -2.60β, which is thus the ''π-only'' vacancy formation energy (note that the π energy of graphite is -3.15β per atom). Coulson *et al.*[11] showed this π-only formation energy should be $-(2.76\pm0.05)\beta$ for an infinite system. Since π bonding is the longest ranged interaction, this appears to vindicate our choice of size of cluster. Hückel theory can reproduce well spectroscopic and calorimetric data of polycyclic aromatic hydrocarbons, but to do so requires different choices of the value of β. Commonly used values for total energies are $\beta=-0.69--0.86$ eV.[27] Hjort *et al.*[16] refitted extra Hückel parameters for the atoms to the vacancy, to reproduce energy levels from a valence effective Hamiltonian method. They concluded that one electron per vacancy must be transferred from the σ to the π system for the D_{3h} vacancy. Also, Pisani *et al.*[15] reported that there is a mixing between the π and the σ systems to an extent that the charge is 0.8 electron higher than obtained by formally assigning one electron per p_z orbital. Our Mulliken orbital analysis confirmed that there is a charge transfer by $0.6e^-$ from the σ to the π system once the relaxed D_{3h} vacancy was formed (but it reverses on forming the C_{2v} vacancy).

2. Density functional theory (DFT)

Now we turn to the symmetry of the DFT MOs. The introduction of a D_{3h} vacancy has no effect on the A_1'' MOs, since these have a node at the vacancy site. The same argument excludes A_2' from the σ system. In a defect molecule approach,[11] the ideal vacancy could be considered as three sp^2 hybrids, giving MOs spanning A_1' and E' and three undercoordinated P_z orbitals, spanning A_2'' and E''. However, in a π system this approach is not helpful, since there are strong interactions with host states of the same symmetry. Figure 2 shows a selected part of the energy level spectrum for the perfect PAH, relaxed symmetric D_{3h} vacancy and relaxed distorted vacancy, with their irreducible representations. There is a strong interaction between the HOMO A_2'' and the other A_2'' once the vacancy is formed, increasing their energy by up to 0.8 eV. It is found that the HOMO is a singly occupied π state and the unoccupied σ doubly degenerate states E' are situated very close to the HOMO (within 20 meV); see Fig. 2.

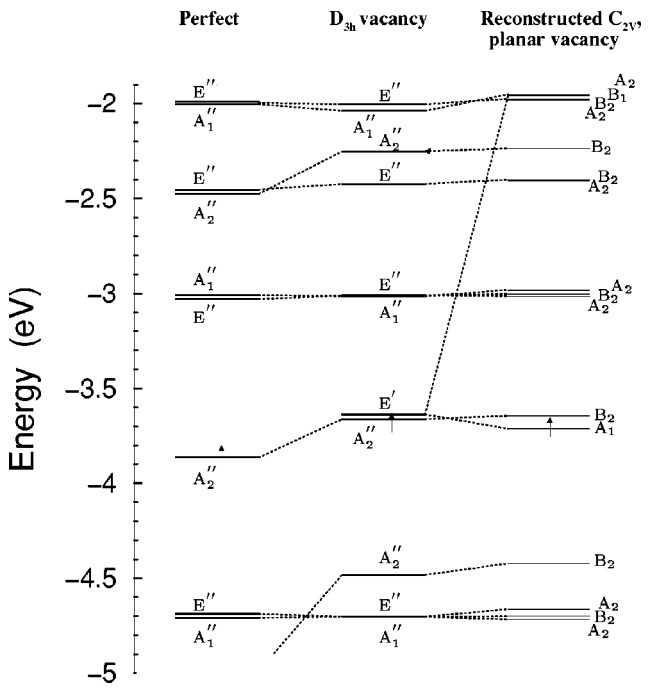

FIG. 2. Kohn-Sham eigenvalues near the Fermi level, for perfect graphene ($C_{121}H_{27}$,D_{3h}), the relaxed symmetric vacancy ($C_{120}H_{27}$,D_{3h}) and the relaxed distorted vacancy ($C_{120}H_{27}$,C_{2v}) with their irreducible representations. Arrows represent the SOMO (singly occupied molecular orbital). Energies are given in eV.

In the defect molecule approach, the $\sigma E'$ state should be occupied by one electron, but this transfers in the symmetric D_{3h} vacancy to the A_2'' π state. Mulliken analysis gives a transfer of $0.6e^-$ from σ to π, the empty $\sigma E'$ state cannot spontaneously distort, but it is only 20 meV above A_2'' π state; once a small distortion is imposed, one of the E' states drops below the A_2'' π state, reversing the charge transfer and facilitating the Jahn-Teller (JT) distortion. Mulliken analysis now gives a π to σ transfer of $0.6e^-$ for the C_{2v} vacancy. As might be expected, the positively charged vacancy does not show a JT distortion, and has the same structure (to within 0.002 Å) as the D_{3h} neutral vacancy. It can be seen in Fig. 3 that the presence of a vacancy defect induces the localization of charge density, resulting in an increase of the energy of

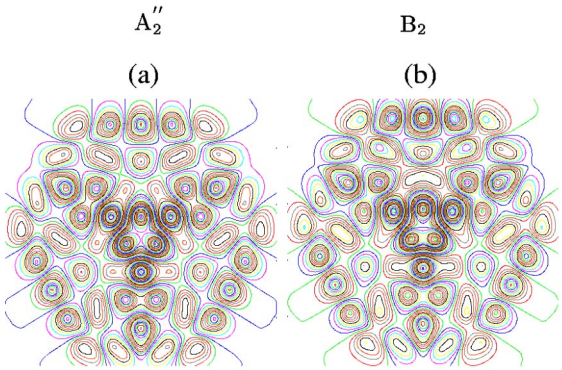

FIG. 3. Contour plots of the symmetric D_{3h} (a) and distorted C_{2v} (b) graphite vacancy wave functions at 1 Å above the molecular plane: parallel to the surface, exhibiting threefold and twofold symmetries, respectively. A_2'' and B_2 are the irreducible representations with energies -4.482 and -4.422 eV for the D_{3h} (a) and C_{2v} (b) vacancies, respectively.

the A_1' and A_2' states. We also plotted the Kohn Sham eigenvalues around the Fermi level for linearly interpolated structures between the relaxed symmetric D_{3h} vacancy and the relaxed distorted vacancy; see Fig. 4. The double degenerate E' σ states split strongly, and the singly occupied A_1 state is lowered in energy, whereas the empty B_1 state jumps by 1.8 eV into the conduction band. It is perhaps surprising that these profound energy level movements are accompanied by only a small change in the total energy.

Graphite systems will normally be expected to be even numbered in order to lower their total energy. We thus examined an even PAH ($C_{112}H_{26}$). The overall structures and energetics were identical to the distorted C_{2v} vacancy in the

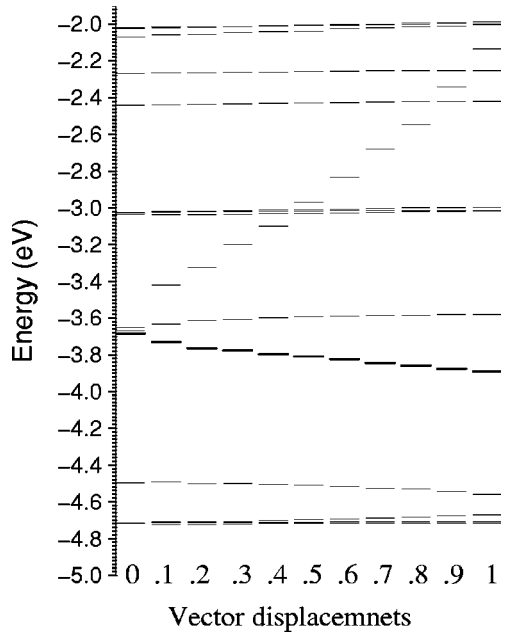

FIG. 4. Kohn-Sham eigenvalues around the Fermi level for linearly interpolated structures between the relaxed symmetric D_{3h} vacancy (0) and the relaxed distorted vacancy (1). The thick lines represent the SOMO.

D_{3h} PAH (to within 0.1 eV and 0.045 Å). The incompatible host molecule symmetry (D_{2h}) splits the $\sigma E'$ state by 0.3 eV in the D_{3h} vacancy structure. However, its splitting upon JT distortion to planar C_{2v} is 1.9 eV (in reverse sense), very similar to the splitting in the D_{3h} host molecule (1.8 eV). Although the $\sigma E'$ state is formally empty, it remains closely correlated with the π HOMO (B_2) state (separated by no more than 0.04 eV in the relaxed distorted C_{2v} vacancy). Fermi occupation statistics cause it to be occupied by $0.5e^-$ and this drives the reconstruction. Self-consistency is impossible to achieve with a step occupation function.

Summarizing our findings, the Jahn-Teller distortion we report here occurs in both the odd alternant D_{3h} host molecule (which is capable of preserving the symmetry of the ideal vacancy) and in the even alternant systems (the D_{2h} host molecule and in supercell calculations). Now we turn to the observation of the vacancy.

C. Dynamics of reconstruction and STM images

Mizes and Foster[28] first made predictive STM images of ''defects'' (isolated adsorbed molecules) on graphite. Such defects are found to perturb the charge density at the Fermi level causing long range electronic perturbations. However, these theoretical predictions were not consistent with any experimental images of the graphite defects using a metal tip. Kelly *et al.*[6] reported that the observed anisotropic scattering patterns only agreed with the predictions of Mizes and Foster when the C_{60} modified tip is used. Recently, Kushmerick *et al.*[4] reported that a narrow distribution of tip electronic states (as in the C_{60} modified tip) is achieved at low temperature. They claimed that the images taken at 77 K of point defects on unsputtered graphite surfaces, which were interpreted as being single vacancies, exhibited anisotropic (threefold) scattering. It is an important fact that STM images can vary due to the type of tip used, the mechanical interactions between the tip and the surface, the temperature and applied bias voltages, and also due to the scan repeats. Theoretical simulations of the vacancy in graphite have been achieved using tight-binding Green's function[29] and *ab initio* periodic Hartree-Fock calculations.[30] Both simulations show a threefold symmetry of the vacancy ground state in graphite. This symmetric view of the vacancy has been widely accepted, in contradiction with our ground state structure and earlier theoretical work.[11,15]

We propose that the accepted threefold symmetry from experimental STM images arises from a time-averaged superposition of the three degenerate states, alternating by the thermally activated dynamic Jahn-Teller effect. We have calculated the energy barrier for the reconstruction to move from one to either of the two other possible reconstructions, related to each other by 120° rotations about the vacancy center. Figure 5 shows an energy diagram for the reconstruction from relaxed D_{3h} for the movement of this reconstruction through the three positions and their related STM images. The barrier for motion is 0.13 eV which, by rudimentary calculation using $f \sim f_D \exp(-\Delta\varepsilon/kT)$, where f_D is the Debye frequency ($\sim 10^{13}$ Hz) gives the cycle frequency, ~65 GHz at room temperature and ~30 kHz at

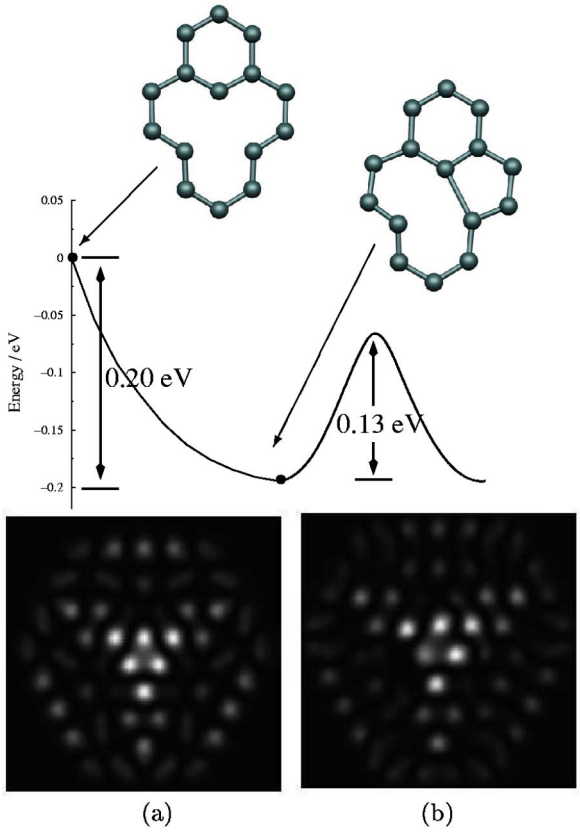

FIG. 5. The energy diagram for the relaxed symmetric D_{3h} and the distorted vacancy. (a) The STM image of the relaxed D_{3h} vacancy. (b) The STM image of one of the three broken symmetry structures; by 120° rotations, of the distorted vacancy. The energy is given relative to the energy of the symmetric D_{3h} vacancy.

liquid nitrogen temperature (~77 K), i.e., 15-ps and 32-μs periods, respectively. On the basis of these calculations we expect the distorted structure to be essentially static as far as STM measurements are concerned below ~55 K (assuming no tip-vacancy interactions). It would be of interest to investigate this prediction by further experiments. The high temperature STM image would thus be expected to show an average of the three possible distorted structures which indeed does have trigonal symmetry; see Figs. 5(a) and 5(b). Also, it is noticed that the perturbation in the wave function decays with the distance from the scattering center.[28]

A further possible effect that may favor obtaining a threefold image is due to the interactions between STM probe tip and the two dangling bonds surrounding the vacancy. These interactions could force whichever atom is nearest the tip to become the dangling bond atom and interact with the tip. In this case, the scanning tunneling microscope breaks the symmetry during traversal and the threefold symmetry of the three positions of the dangling carbon atoms would still be observed.

D. Formation and migration energies

The formation energy of the distorted ground-state structure, E_f^v for the $C_{120}H_{27}$ graphene sheet using the method of Badziag *et al.*,[31] was 7.4 eV. The formation energy we arrive at agrees well with the experimental value, 7.0 ± 0.5 eV (Ref. 32) and earlier semiempirical and local density approximation (LDA) results of 7.3 eV (Ref. 17) and 7.6 eV,[18] respectively. Using a relaxation constrained by symmetry, we have calculated the migration path for a vacancy to move to a neighboring atomic site. The saddle point or energy barrier to migration was calculated for the cluster $C_{111}H_{26}$ relaxed under C_{2v} symmetry, and was found to be 1.7 eV. The saddle point structure is shown in Fig. 6(a). These findings broadly agree with earlier theoretical results, 1.6 eV from first principles (LDA) (Ref. 18) and 1.4 eV obtained using the tight-binding level of theory, but significantly, the value is well below that obtained through some experiments, $\sim 3.1 \pm 0.5$ eV.[32] No previous comment has been made on this discrepancy and some justification of the low theoretical value is therefore required.

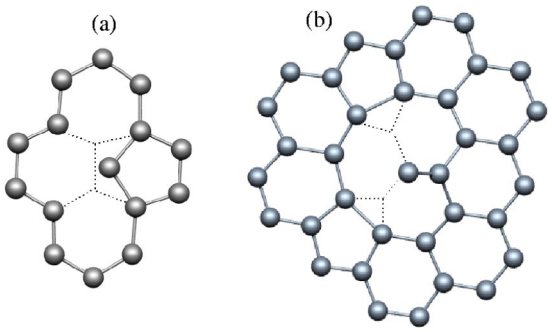

FIG. 6. The saddle points for motion of the planar monovacancy (a) and coplanar divacancy (b).

We note that the value of 3.1 eV for the migration energy of monovacancies in graphite was obtained from TEM observations made on the temperature of appearance ~650 °C, and kinetics of growth of microscopic vacancy clusters[8] in irradiated graphite. The assumption is that the rate at which these clusters grow is dictated by the in-plane migration energy of vacancies to the cluster nucleus. It is essential to note that there are other possible vacancy-type defects that would form under irradiation and produce the same net result but migrate at higher energies. Therefore we considered various vacancy-type species. We first looked at divacancies, since these were expected to be more stable and less mobile than the single vacancy. The di-vacancy is formed when two neighboring vacancies coalesce, the lowest energy state of which is when this occurs in the same atomic layer. The defect is planar with strongly reconstructed bonds, enclosing two opposing fivefold rings and a shared eightfold ring, $E_f = 8.7$ eV. However, using a similar method to that used to calculate monovacancy migration, we found that $E_m^{v_2}$ is approximately 7 eV [see Fig. 6(b)], eliminating the possibility that this defect was being observed in the experiments.

We propose that the accepted experimental migration energy derives from an aggregate of processes, including the recently reported vacancy trapping.[33] This can occur through formation of range of metastable interplanar divacancies when two vacancies approach one another in *neighboring* sheets. The displacement of atoms out of plane, described

earlier, is believed to facilitate this process. This type of divacancy is more mobile than its coplanar counterpart and is formed by strong (single or double bond) covalent interactions between graphite layers. These defects act as traps that constrain vacancy migration, and the process of vacancy transport is now either controlled by complete detrapping or movement between inter-planar traps, in addition to the 1.7 eV for monovacancy migration E_m^v, leading to a net value in the region of $\sim$3.2–3.6 eV.[33] In heavily irradiated graphites, mutual trapping will be expected to limit the rate of the overall transport process, thus explaining why the observed value is higher than that for the single vacancy process. This highlights the importance of the (to our knowledge) previously unreported out-of-plane Jahn-Teller displacement since it allows the atoms to take part in cross-layer interactions more readily than if the atoms lay in plane. The experimental cluster growth measurements referred to above[8] were conducted on quite heavily irradiated graphite with, one would expect, a correspondingly large population of vacancies, making trapping highly probable. In view of this, the net migration energy associated with transport of vacancies in irradiated graphite should be a function of concentration and tend to our value if the concentration is very small. This interpretation vindicates the previously surprising observations of Hinman *et al.*[34] They found that in lightly irradiated graphite, the concentration of defects carefully identified by etching, as monovacancies, starts to drop rapidly with increasing temperature, presumably due to migration and subsequent aggregation, within a temperature regime well below that at which it was considered possible, given the accepted figure for E_m^v. Further supporting evidence in favor of a low or variable migration energy has been given recently by Asari *et al.*[35] who report Raman measurements of the damage relaxation processes, suggesting that vacancy motion is associated with an energy of $\sim 1.8 \pm 0.3$ eV. We therefore have confidence in suggesting that the low value should replace the commonly accepted value in lightly irradiated specimens. In particular, since there are no interlayer interactions in single walled nanotubes, the lower migration energy of vacancies should apply there, but perhaps slightly higher due to the anticipated stronger reconstruction effect mentioned earlier.

IV. CONCLUSION

First principles calculations on the vacancy in graphite have identified some important new insights into vacancy structure and electronic behavior. Particularly, we highlight the previously unreported behavior that is a consequence of the symmetry-breaking (Jahn-Teller) distortion and lowering the energy further (0.2 eV). This distortion includes a partially reconstructed bond, 2.1 ± 0.1 Å, resulting in the formation of a closed five-fold ring and displacement of the remaining unsaturated atom out of the plane. This last feature of the distortion increases interaction of the vacancy with other defects, which in turn affects its migration energy, solving the riddle of the low theoretical calculations of the migration energy by involving less mobile metastable interplanar di-vacancies. We also discussed our structural model of the vacancy in relation to predicted and experimental STM images, and found our results consistent with observation.

*Present address: CPES, Dept. of Chemistry, University of Sussex, Falmer, Brighton, BN1 9QJ, Sussex, United Kingdom.
Electronic address: a.a.e.el-barbary@sussex.ac.uk

[1] F. Banhart, Rep. Prog. Phys. **62**, 1181 (1991).
[2] Q. M. Zhang, H. K. Kim, and M. H. W. Chan, Phys. Rev. B **33**, 413 (1986).
[3] P. M. Ajayan, V. Ravikumar, and J. C. Charlier, Phys. Rev. Lett. **81**, 1437 (1998).
[4] J. G. Kushmerick, K. F. Kelly, H.-P. Rust, N. J. Halas, and P. S. Weiss, J. Phys. Chem. B **103**, 1619 (1999).
[5] J. R. Hahn and H. Kang, Phys. Rev. B **60**, 6007 (1999).
[6] K. F. Kelly, D. Sarkar, G. D. Hale, S. J. Oldenburg, and N. J. Halas, Science **273**, 1371 (1996).
[7] Z. Tang, M. Hasegawa, T. Shimamura, Y. Nagai, T. Chiba, Y. Kawazoe, and M. Takenaka, Phys. Rev. Lett. **82**, 2532 (1999).
[8] P. A. Thrower, Chem. Phys. Carbon **5**, 217 (1969).
[9] G. J. Dienes, J. Appl. Phys. **23**, 1194 (1952).
[10] R. L. Wooley, Nature (London) **197**, 66 (1963).
[11] C. A. Coulson, M. A. Herraez, M. Leal, E. Santos, and S. Senent, Proc. R. Soc. London, Ser. A **274**, 461 (1963).
[12] C. A. Coulson and M. D. Poole, Carbon **2**, 275 (1964).
[13] A. P. P. Nicholson and D. J. Bacon, Carbon **13**, 275 (1975).
[14] A. Zunger and R. Englman, Phys. Rev. B **17**, 642 (1978).
[15] C. Pisani, R. Dovesi, and P. Carosso, Phys. Rev. B **20**, 5345 (1979).
[16] M. Hjort and S. Stafström, Phys. Rev. B **61**, 14 089 (2000).
[17] C. H. Xu, C. L. Fu, and D. F. Pedraza, Phys. Rev. B **48**, 13 273 (1993).
[18] E. Kaxiras and K. C. Pandey, Phys. Rev. Lett. **61**, 2693 (1988).
[19] A. V. Krasheninnikov, K. Nordlund, M. Sirvio, E. Salonen, and J. Keinonen, Phys. Rev. B **63**, 245405 (2001).
[20] P. R. Briddon and R. Jones, Phys. Status Solidi B **217**, 131 (2000).
[21] P. Hohenberg and W. Kohn, Phys. Rev. **136**, 864 (1964).
[22] W. Kohn and L. J. Sham, Phys. Rev. **140**, 1133 (1965).
[23] G. B. Bachelet, D. R. Hamann, and M. Schlüter, Phys. Rev. B **26**, 4199 (1982).
[24] J. Tersoff and D. R. Hamann, Phys. Rev. B **31**, 805 (1985).
[25] M. D. Segall, P. L. D. Lindan, M. J. Probert, C. J. Pickard, P. J. Hasnip, S. J. Clark, and M. C. Payne, J. Phys.: Condens. Matter **14**, 2717 (2002).
[26] M. Fujita *et al.*, J. Phys. Soc. Jpn. **65**, 1920 (1996).
[27] A. Streitwieser, *Molecular Orbital Theory for Organic Chemists* (Wiley, New York, 1961).
[28] H. A. Mizes and J. S. Foster, Science **244**, 559 (1989).
[29] A. V. Krasheninnikov and V. F. Elesin, Surf. Sci. **455–456**, 519 (2000).
[30] K. H. Lee, M. Causa, S. S. Park, C. Lee, Y. Suh, H. M. Eun, and D. Kim, J. Mol. Struct.: THEOCHEM **506**, 297 (2000).
[31] P. Badziag, W. S. Verwoerd, W. P. Ellis, and N. R. Greiner, Nature (London) **343**, 244 (1990).

[32] P. A. Thrower and R. M. Mayer, Phys. Status Solidi A **47**, 11 (1978).
[33] R. H. Telling, C. P. Ewels, A. A. El-Barbary, and M. I. Heggie, Nat. Mater. **2**, 333 (2003).
[34] G. W. Hinman, A. Haubold, J. O. Gardner, and J. K. Layton, Carbon **8**, 341 (1970).
[35] E. Asari, M. Kitajima, K. G. Nakamura, and T. Kawabe, Phys. Rev. B **47**, 11 143 (1993).